Spectroscopic investigation of coupling among asymmetric InGaN/GaN multiple quantum wells grown on non-polar a-plane GaN substrates

A. T. Roberts, A. Mohanta, H. O. Everitt, J. H. Leach, D. Van Den Broeck et al.

Citation: Appl. Phys. Lett. **103**, 181106 (2013); doi: 10.1063/1.4827536
View online: http://dx.doi.org/10.1063/1.4827536
View Table of Contents: http://apl.aip.org/resource/1/APPLAB/v103/i18
Published by the AIP Publishing LLC.

Spectroscopic investigation of coupling among asymmetric InGaN/GaN multiple quantum wells grown on non-polar a-plane GaN substrates

A. T. Roberts,[1] A. Mohanta,[2] H. O. Everitt,[1,3] J. H. Leach,[4] D. Van Den Broeck,[5] A. M. Hosalli,[5] T. Paskova,[5,a)] and S. M. Bedair[5]
[1]*U.S. Army Aviation and Missile Research, Development, and Engineering Center, Redstone Arsenal, Alabama 35898, USA*
[2]*Oak Ridge Institute for Science and Education, Research Participation Program, U.S. Army Aviation and Missile Research, Development and Engineering Center, Redstone Arsenal, Alabama 35898, USA*
[3]*Department of Physics, Duke University, Durham, North Carolina 27708, USA*
[4]*Kyma Technologies, Raleigh, North Carolina 27617, USA*
[5]*Department of Electrical and Computer Engineering, North Carolina State University, Raleigh, North Carolina 27695, USA*

(Received 23 September 2013; accepted 13 October 2013; published online 29 October 2013)

Low defect density asymmetric multiple quantum wells (MQWs) of InGaN/GaN grown on non-polar a-plane GaN substrates were investigated using time-integrated and time-resolved photoluminescence spectroscopy. Comparison of these spectra with the predicted emission energies reveals that these QWs may be spectrally resolved at low temperatures. However, a combination of thermal activation and resonant tunneling of carriers increasingly coupled the QWs, favoring emission from the lowest energy QWs with increasing temperature in a manner analogous to MQWs composed of other non-polar semiconductor materials but unlike most InGaN MQWs grown on polar substrates and influenced by the strong polarization-dependent effects. © *2013 AIP Publishing LLC*. [http://dx.doi.org/10.1063/1.4827536]

During the last 20 years, violet, blue, and green light emitting diodes (LEDs) and laser diodes (LDs) based on InGaN quantum well (QW) structures have been demonstrated with a steady improvement of their performance.[1,2] InGaN/GaN coupled QW structures are known to improve device performance by facilitating carrier transport within the active region, dramatically increasing the light-output power of the devices at high current density.[3,4] However, despite intensive research on stress and defect generation, polarization fields, localization of charge carriers, exciton binding, confinement of the charge carriers by the QW barriers, and delocalization of charge carriers apart from nonradiative recombination centers, no approach adequately explains how these factors combine to affect nonradiative recombination and reduce device efficacy.[5,6]

Almost all research on InGaN/GaN symmetric and asymmetric QWs has been of polar material grown in the c-direction with strong polarization and piezoelectric effects.[3,4] Although these effects may be minimized in LED structures if the QWs are fabricated in non-polar orientations, there have been few such investigations, including studies of (11-20) "a-plane" InGaN/GaN QWs on (10-12) r-plane sapphire and a-plane SiC as well as studies of (10-10) "m-plane" InGaN/GaN QWs on (100) $LiAlO_2$ substrates.[7–9] In a prototypical study, the reduced quantum-confined Stark effect in a-plane GaN/AlGaN QW structures reduced the redshift with increasing QW width as compared to structures grown in the c-direction.[10] However, these QWs, grown on a film of a-plane GaN on r-plane sapphire, possessed a high defect density of both dislocations and stacking faults. Heteroepitaxially grown non-polar InGaN/GaN QW structures are characterized by presence of an even higher density of dislocations and stacking faults due to the large lattice mismatch with the available substrates.[11] By contrast, reduced defect density lateral epitaxial overgrown a-plane InGaN/GaN QWs exhibited no shift in their electroluminescence peak with drive current.[12]

Of course the ideal solution to reduce the defect density would be to employ low-defect density, non-polar bulk GaN substrates.[13,14] Even though the crystalline quality of non-polar substrates has improved dramatically in such homoepitaxial structures, the efficiency of non-polar LED devices remains quite low, and there has been no report investigating the growth and dynamics of tailored or asymmetric non-polar QW structures. Here, we present an investigation of a low defect density, non-polar, asymmetric-coupled InGaN QW structure grown on an a-plane GaN substrate. Temperature dependent time-integrated and time-resolved photoluminescence (TIPL and TRPL) spectra were used to resolve the QW emission and investigate the carrier transport among the coupled QWs. We find a combination of thermal activation and resonant tunneling of carriers increasingly coupled the QWs, favoring emission from the lowest energy QWs with increasing temperature in a manner analogous to multiple QWs (MQWs) composed of other non-polar semiconductor materials such as GaAs.

The non-polar a-plane (11–20) GaN substrate was obtained by vertically slicing a low dislocation density (5×10^5–2×10^6 cm^{-2}) GaN boule grown along the polar c-plane (0001) direction. The MQW structure was grown on this substrate in a vertical flow metal-organic chemical vapor deposition (MOCVD) reactor designed to operate in two modes: a 2-column flow mode (Fig. 1(a)), and a 1-column flow mode (Fig. 1(b)). In both modes, the substrate rotates at a speed of 60 rpm. In the 2-column flow mode, only half the sample area is exposed to the MO flux at any instant, and it is

a)Author to whom correspondence should be addressed. Electronic mail: tmpaskov@ncsu.edu. Tel.: 919.513.3124. Fax: 919.515.2545.

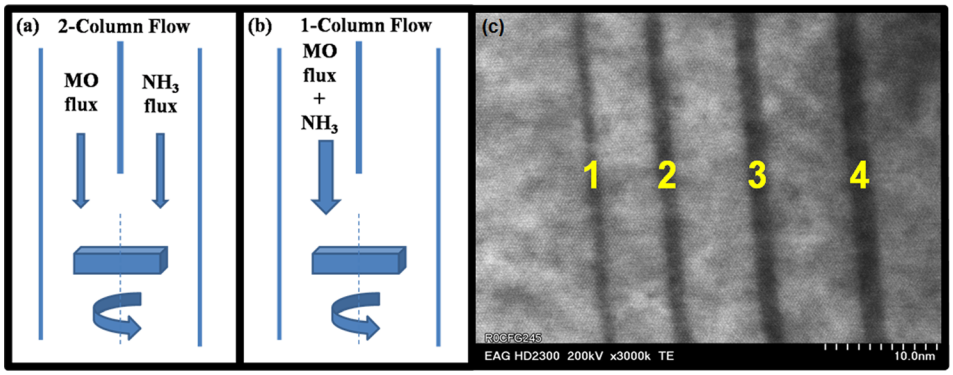

FIG. 1. (a) One- and (b) two-column growth mode technique. (c) A representative TEM image of the MQW structure with each QW labeled.

there that Ga and In atoms are physically adsorbed on the surface. The probability of chemical adsorption and bond formation of these atoms becomes highest after the sample rotates 180° and comes under the influence of the NH_3 flux. The very small surface residence lifetime of In produces strong desorption during rotation and limits its incorporation into the QWs, but in 1-column flow, the entire sample area experiences both the MO flux and the NH_3 flux simultaneously so the percentage of In incorporation is higher.

The bulk GaN substrates were initially etched *in situ* for 2 min at 980 °C in an atmosphere of H_2 and NH_3. Deposition on these substrates was then carried out in the 2-column flow mode with a system pressure of 350 mTorr and a trimethylgallium (TMGa) source producing a V-III ratio of 7700. First, a 750 nm layer of intrinsic GaN was deposited, followed by a 2.5 μm n-type layer of GaN:Si deposited at 975 °C. Next, the reactor was switched to a 1-column flow mode for the MQWs using sources of triethylgallium (TEGa) and trimethylindium (TMIn) whose ratios were established with mass flow controllers as described previously.[15] Four $In_xGa_{1-x}N$/GaN QWs (labeled 1-4) were fabricated at 620/650 °C with a higher flow of NH_3 that doubled the V-III ratio. Subsequent energy dispersive x-ray spectroscopy indicated the In composition of the QWs varied from x = 0.10–0.12. The quantum well/quantum barrier thicknesses measured by transmission electron microscopy (TEM) varied as 1.0/5.5, 1.4/6.7, 1.7/7.2, and 1.9/15 nm for QWs 1-4, respectively (Fig. 1(c)). After MQW fabrication, the reactor was switched back to the original 2-column mode, and the deposition concluded with a 100 nm capping layer of intrinsic GaN. None of the TEM imagery, including that shown in Fig. 1(c), revealed any stacking faults in the QW region, but evidence for some stacking faults in other GaN regions will be presented shortly.

The energy levels of the a-plane $In_xGa_{1-x}N$/GaN QWs can be estimated using $E_{InGaN} = E_R + E_S + E_Q$ for the relaxed, strained, and quantum confined contributions, respectively. The first term $E_R = (1-x)E_G^{GaN} + xE_G^{InN} - bx(1-x)$ is expressed as a function of the InN percentage (x), the InN band gap ($E_G^{InN} = 0.692$ eV at 2 K), the GaN band gap ($E_G^{GaN} = 3.503$ at 1.6 K), and the bowing parameter b.[16–18] For InGaN/GaN QWs thinner than the critical layer thickness for relaxation, the band gap will be blue shifted due to compressive strain as $E_S = -14.22\varepsilon_{xx} - 51.603\varepsilon_{xx}^2$, where $\varepsilon_{xx} = (a_{GaN} - a_{InGaN})/a_{InGaN} = -0.0193$ was estimated from measured lattice constants.[16,19] Finally, the Kronig-Penney model was used to estimate the quantum size effect that increases the energy within the QWs as the width decreases. Figure 2 summarizes the predicted emission energies as a function of QW width for In compositions $x = 8\%$, 10%, and 12% using a bowing parameter ($b = 2.0$ eV) consistent with previously reported values.[16,20]

Temperature-dependent TIPL and TRPL spectra from the QWs are generated using pulsed excitation at 350 nm from an optical parametric amplifier driven by an amplified 800 nm mode-locked fiber laser with a 1 kHz repetition rate. The pulse duration was 130 fs, and the fluence on the sample was 70 μJ/cm^2. Temperature dependent TIPL spectra were measured with a 30 cm grating spectrometer and a Princeton Instruments Spec-10 liquid nitrogen cooled detector, and TRPL spectra were measured with a Hammamatsu C4334 streak camera. In both measurements, the sample was mounted in a closed-cycle helium cryostat. Fig. 3(a) compares the 45 K TIPL spectra of the MQW sample and the substrate. The high density of stacking faults in a-plane GaN epilayers are known to produce emission peaks in the PL spectra,[21–23] and the feature observed at 3.471 eV matches the donor bound exciton transition (3.4709 eV) of bulk and homoepitaxial GaN samples grown by MOCVD on strain-free bulk GaN substrates.[24] In addition, Liu *et al.*[21] have established a direct correlation between structural features associated with stacking faults and emission peaks in the range of 3.29–3.41 eV. Our PL spectrum reveals two such narrow peaks, located at 3.35 eV and 3.393 eV. The remaining broad emission peaks are associated with the MQW. Although the sample contains four QWs, only three

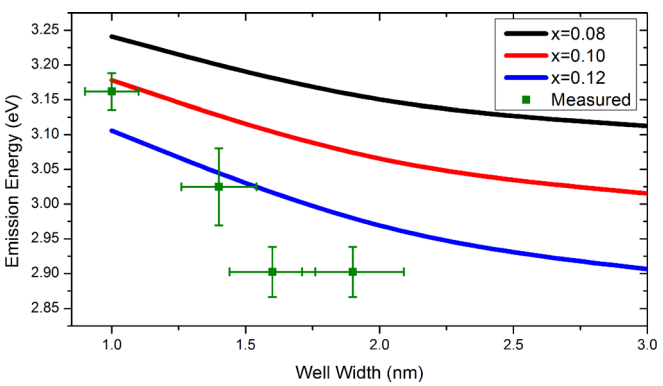

FIG. 2. Calculated emission energy as a function of QW width for different In concentrations x assuming b = 2.0 eV and T = 12 K. The green squares represent measured TIPL QW emission averaged over many locations on the sample. The horizontal error bars represent a 10% uncertainty in QW thickness.

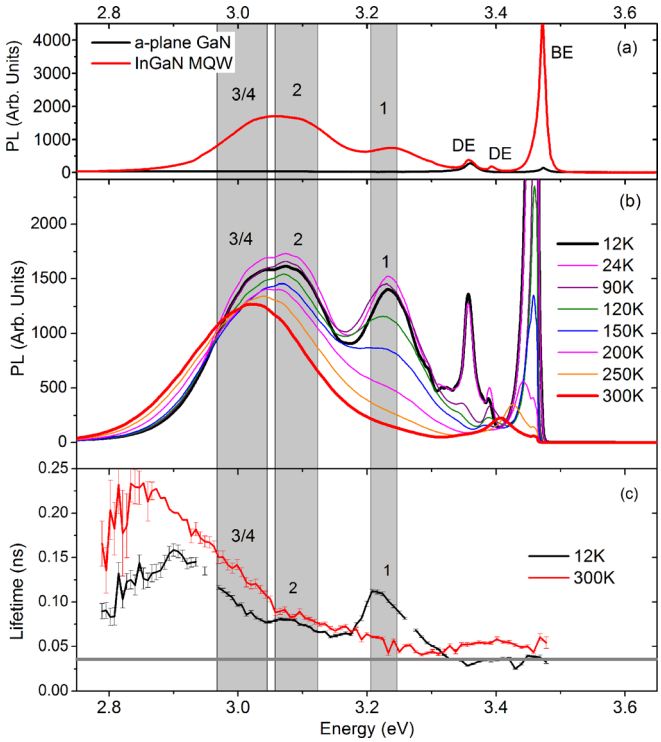

FIG. 3. (a) TIPL spectra taken at 45 K for a-plane GaN substrate (black) and InGaN MQW (red). The peak labeled BE is attributed to bound excitons, DE indicates defect related emission, and 1, 2, 3/4 indicates QW emission. The grey regions represent the site-to-site spectral variation in emission peak location for different spatial sites. (b) Temperature sequenced TIPL for InGaN MQW from 12 K to 300 K. (c) TRPL lifetime spectra for the dominant, faster decaying component measured at 12 K (black) and 300 K (red). The horizontal line at 30 ps indicates the instrument limited temporal response.

peaks are observed because the widths of QWs 3 and 4 are similar enough that their PL emission overlaps at all temperatures.

The peak QW energies obtained through measurements of the 12 K TIPL spectra overlay the predictions (Fig. 2) so that the dependence of QW energy on QW width and In composition may be explored. The vertical error bars represent the standard deviation of the emission peaks at different locations across the sample, suggesting a ~10% variation in the QW thickness and perhaps In concentration. Beyond these small spatial variations, Fig. 2 indicates the percentage of In incorporated in the QWs evolved during the deposition from about 10% in QW1 to at least 12% for the other QWs.

Temperature-dependent TIPL and TRPL were used to assess the degree to which coupling occurs among the individual QWs. The temperature-dependent TIPL spectra in Fig. 3(b) shows that QW1 emission decreases in intensity and broadens with increasing temperature, especially above 120 K where the observed PL thermal quenching behavior can be explained by thermal escape or thermally activated nonradiative recombination. An Arrhenius plot of the emission intensity from QW1 (Fig. 4) reveals an activation energy of 34 ± 8 meV for this thermal quenching. However, the emission intensity increases from 12 to 50 K, suggesting a different thermal activation process frees carriers from nonradiative traps at low temperatures.

In addition to these thermally activated mechanisms, carriers can tunnel between the QWs in a temperature-

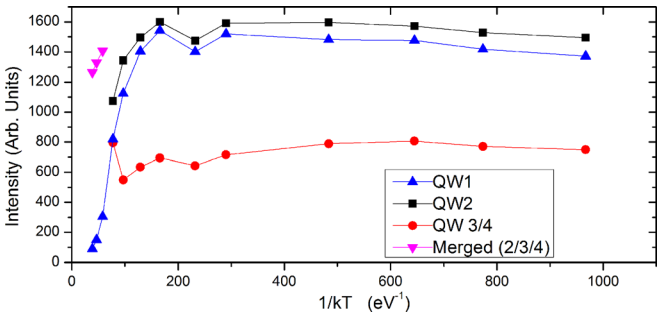

FIG. 4. Temperature dependence of PL intensities from the various MQW emission peaks.

dependent manner. The temperature dependence of the peaks 2 and 3/4, fit with a sum of two Gaussian lineshape functions, showed little change in temperature until 150 K, at which point the two features merge into one PL band that survives to room temperature (Fig. 4). Additionally, the lower energy side of the merged PL band shown in Fig. 3(b) begins to increase substantially above 150 K, indicating that thermal activation allows QW3 and QW4 to gain additional carriers for radiative recombination. It is well understood that the coupling between adjacent QWs increases substantially under resonant tunneling conditions.[25] The disappearance of the QW2 emission near 150 K, in contrast with the resilience of the QW3/4 emission (Fig. 4), suggests the onset of resonant tunneling and significant carrier injection from QW2 into QW3 and QW4. Such a tunneling behavior has also been observed in asymmetric coupled multi-quantum wells of AlAs/AlGaAs and GaAs/AlAs.[25]

Because it was often difficult to resolve the TIPL spectra from the contributed QWs, TRPL measurements were performed in hopes of resolving the QWs temporally. Figure 5 illustrates a typical TRPL trace for a small portion of the spectrum, overlaid by a biexponential fit from which fast and slow decay time constants were obtained. The rapidly decaying component, characterized by a 30–200 ps time constant, accounted ~85% of the amplitude, while the slower component with a time constant of 0.5–2.5 ns accounted for the rest. The TRPL spectra were analyzed in this manner over successive emission energy windows of 1 nm width (~8 meV) across the entire QW spectrum. The lifetime spectrum in Fig. 3(c) represents a plot of the dominant, faster decaying component for each emission energy at two temperatures, 12 K and 300 K. In the 12 K spectrum, there are three peaks which correspond to the three distinguishable

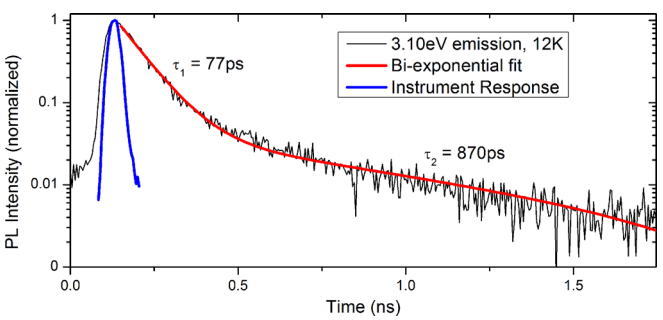

FIG. 5. A representative TRPL decay curve of MQW emission at 12 K over an 8 meV window centered at 3.10 eV (black). The fitting function is a bi-exponential decay (red), and the instrumental response function is shown in blue.

QWs. Because the emission decay lifetime varies as a function of confined carrier energy, the coolest carriers at the bottom of the QW decay most slowly, while successively hotter carriers decay faster through a combination of radiative decay and nonradiative cooling toward the bottom of the QW. Thus, the peak energies in the TRPL lifetime spectrum, which are close to those seen in the TIPL of Fig. 3(b), correspond to the bottom of a QW.

The temperature dependence of the lifetime spectrum reveals that the decay of QW1 emission accelerates as temperature rises, a behavior characteristic of thermally activated nonradiative recombination (Fig. 3(c)). Conversely and simultaneously, the decay rate of the QW3/4 emission slows as temperature rises, clearly indicating that these QWs are coupled and that carriers are tunneling from the high energy QWs to the lower energy QWs via thermally activated channels. With increasing temperature (Fig. 4), relatively fewer carriers remain in the QW1 and QW2 to recombine radiatively as more carriers tunnel to the lower energy QWs, thus, explaining the differing temperature-dependent behavior of the QWs (Fig. 4). These findings are in stark contrast to the behavior observed in the temperature-dependent PL spectra of polar, coupled, asymmetric InGaN/GaN QWs where resonant tunneling transfers carriers from the wider to the narrower QWs.[26] There, the emission efficiency of the narrow QW is enhanced, while our measurements on non-polar substrates confirms the emission efficiency of the wider QW is enhanced just as it is in conventional, non-polar MQW structures in other semiconductor systems.

This research was supported in part by appointment of A.M. to the Postgraduate Research Participation Program at the U.S. Army Aviation and Missile Research, Development and Engineering Center administered by the Oak Ridge Institute for Science and Education through an interagency agreement with the U.S. Department of Energy, as well as by National Science Foundation (Nos. DMR-1105842 and DMR-1207075).

[1]S. Nakamura, T. Mukai, and M. Senoh, Appl. Phys. Lett. **64**, 1687–1689 (1994).
[2]K. S. Kim, J. K. Son, S. N. Lee, Y. J. Sung, H. S. Paek, H. K. Kim, M. Y. Kim, K. H. Ha, H. Y. Ryu, O. H. Nam, T. Jang, and Y. J. Park, Appl. Phys. Lett. **92**, 101103 (2008).
[3]X. Ni, Q. Fan, R. Shimada, Ü. Özgür, and H. Morkoç, Appl. Phys. Lett. **93**, 171113 (2008).
[4]J.-Y. Zhang, L.-E. Cai, B.-P. Zhang, X.-L. Hu, F. Jiang, J.-Z. Yu, and Q.-M. Wang, Appl. Phys. Lett. **95**, 161110 (2009).
[5]A. Hangleiter, D. Fuhrmann, M. Grewe, F. Hitzel, G. Klewer, S. Lahmann, C. Netzel, N. Riedel, and U. Rossow, Phys. Status Solidi A **201**, 2808–2813 (2004).
[6]C. Netzel, V. Hoffmann, T. Wernicke, A. Knauer, M. Weyers, M. Kneissl, and N. Szabo, J. Appl. Phys. **107**, 033510 (2010).
[7]A. Chitnis, C. Chen, V. Adivarahan, M. Shatalov, E. Kuokstis, V. Mandavilli, J. Yang, and M. A. Khan, Appl. Phys. Lett. **84**, 3663–3665 (2004).
[8]T. S. Ko, T. C. Lu, T. C. Wang, M. H. Lo, J. R. Chen, R. C. Gao, H. C. Kuo, S. C. Wang, and J. L. Shen, Appl. Phys. Lett. **90**, 181122 (2007).
[9]P. Waltereit, O. Brandt, A. Trampert, H. T. Grahn, J. Menniger, M. Ramsteiner, M. Reiche, and K. H. Ploog, Nature **406**, 865–868 (2000).
[10]M. D. Craven, P. Waltereit, J. S. Speck, and S. P. DenBaars, Appl. Phys. Lett. **84**, 496 (2004).
[11]S. Chichibu, T. Azuhata, T. Sota, and S. Nakamura, Appl. Phys. Lett. **69**, 4188–4190 (1996).
[12]A. Chakraborty, B. A. Haskell, S. Keller, J. S. Speck, S. P. DenBaars, S. Nakamura, and U. K. Mishra, Appl. Phys. Lett. **85**, 5143 (2004).
[13]T. Detchprohm, M. Zhu, Y. Li, Y. Xia, C. Wetzel, E. A. Preble, L. Liu, T. Paskova, and D. Hanser, Appl. Phys. Lett. **92**, 241109 (2008).
[14]X. Li, X. Ni, J. Lee, M. Wu, Ü. Özgür, H. Morkoç, T. Paskova, G. Mulholland, and K. R. Evans, Appl. Phys. Lett. **95**, 121107 (2009).
[15]P. T. Barletta, E. A. Berkman, B. F. Moody, N. A. El-Masry, A. M. Emara, M. J. Reed, and S. M. Bedair, Appl. Phys. Lett. **90**, 151109 (2007).
[16]A. M. Emar, E. A. Berkman, J. Zavada, N. A. El-Masry, and S. M. Bedair, Phys. Status Solidi C **8**, 2034–2037 (2011).
[17]B. Monemar, Phys. Rev. B **10**, 676 (1974).
[18]B. Arnaudov, T. Paskova, P. P. Paskov, B. Magnusson, E. Valcheva, B. Monemar, H. Lu, W. Schaff, H. Amano, and I. Akasaki, Phys. Rev. B **69**, 115216 (2004).
[19]M. J. Reed, N. A. El-Masry, C. A. Parker, J. C. Roberts, and S. M. Bedair, Appl. Phys. Lett. **77**, 4121–4123 (2000).
[20]E. Sakalauskas, O. Tuna, A. Kraus, H. Bremers, U. Rossow, C. Giesen, M. Heuken, A. Hangleiter, G. Gobsch, and R. Goldhahn, Phys. Status Solidi B **249**, 485–488 (2012).
[21]R. Liu, A. Bell, F. A. Ponce, C. Q. Chen, J. W. Yang, and M. A. Khan, Appl. Phys. Lett. **86**, 021908 (2005).
[22]J. Lähnemann, O. Brandt, U. Jahn, C. Pfüller, C. Roder, P. Dogan, F. Grosse, A. Belabbes, F. Bechstedt, A. Trampert, and L. Geelhaar, Phys. Rev. B **86**, 081302 (2012).
[23]P. P. Paskov, R. Schifano, T. Paskova, B. Monemar, S. Figge, and D. Hommel, J. Appl. Phys. **98**, 093519 (2005).
[24]B. Monemar, J. Phys.: Condens. Matter **13**, 7011 (2001).
[25]G. Livescu, A. M. Fox, D. A. B. Miller, T. Sizer, W. H. Knox, A. C. Gossard, and J. H. English, Phys. Rev. Lett. **63**, 438–441 (1989).
[26]Y. Wang, X. J. Pei, Z. G. Xing, L. W. Guo, H. Q. Jia, H. Chen, and J. M. Zhou, Appl. Phys. Lett. **91**, 061902 (2007).